STATIC CAPACITY PREDICTION BY DYNAMIC METHODS FOR THREE BORED PILES

By Jean-Louis Briaud,[1] Fellow, ASCE, Marc Ballouz,[2] and George Nasr,[3] Members, ASCE

ABSTRACT: Three bored piles were built and tested at the National Geotechnical Experimentation Sites, at Texas A&M University, to gather data on the reliability of large-strain dynamic methods to predict the static capacity of bored piles. The three piles had a nominal diameter of 0.915 m, a nominal length of 10 m, and some planned and unplanned defects. The piles were first subjected to a static load test and then four companies were asked to perform dynamic tests—namely, Statnamic and drop weight tests—and predict the static load test results. The paper shows the comparison between predicted and measured results.

INTRODUCTION

Bored piles are a very popular and cost-effective type of foundation. The major objective of this project was to evaluate the ability of large-strain dynamic testing methods—namely, the drop weight method and the Statnamic method—to predict the static capacity of bored piles. This objective was achieved by constructing two bored piles in sand and one bored pile in clay at the National Geotechnical Experimentation Sites at Texas A&M University, inviting various companies to perform large-strain dynamic testing (drop weight and Statnamic) and make "class A" predictions of the static capacity of the three bored piles; this static capacity was measured by conventional static load tests. Similar tests were performed in California prior to the Texas A&M University tests, but, for the California tests, the predicting companies knew the load test results before making their predictions. These predictions are, therefore, not "class A" predictions and are not reported here. They can be found in Baker et al. (1993). That reference also includes the Texas A&M University tests.

SITE AND SOIL DESCRIPTION

The sites were the two National Geotechnical Experimentation Sites at Texas A&M University: Sand and Clay. The top layers, 12.5 m at the sand site and 6.5 m at the clay site, are 100,000-year-old river deposits, while the hard clay underlying both sites is a 45,000,000-year-old marine shale that was deposited by a series of transgressions and regressions of the Gulf of Mexico. The sand is a medium-dense silty sand with the properties shown in Fig. 1(a). The clay is a very stiff plastic clay with the properties shown in Fig. 1(b). Details of the soil properties are in Briaud (1997) and Simon and Briaud (1996).

BORED PILES CONSTRUCTION

A total of nine bored piles were constructed, piles 1–5 at the sand site and piles 6–9 at the clay site. All piles were planned to be 0.915 m in diameter and varied in length between 10.7 and 24.1 m. At the clay site the piles were drilled dry while at the sand site they were drilled dry to start and then completed under slurry. Details of the construction are in Ballouz et al. (1991) and the construction schedule is given in Table 1. This table also gives the testing sequence for each pile. The piles were constructed by following good drilling and construction practices including desanding of the drilling mud and minimizing slurry stagnation between the end of drilling and the beginning of concreting. Pile 2 at the sand site was an exception.

Pile 2 (Fig. 2) at the sand site was purposely built with a mud cake on the side wall, a soft bottom, and a concrete contamination at 5.3 m below the top of the pile. The mud cake was approximately 15 mm thick and was created by leaving the bentonite drilling mud in the open hole for 60 h; the mud cake was extremely slick. The soft bottom was created when the sand mixed with the drilling slurry settled at the bottom of the hole during the 60 h and formed an approximately 0.3-

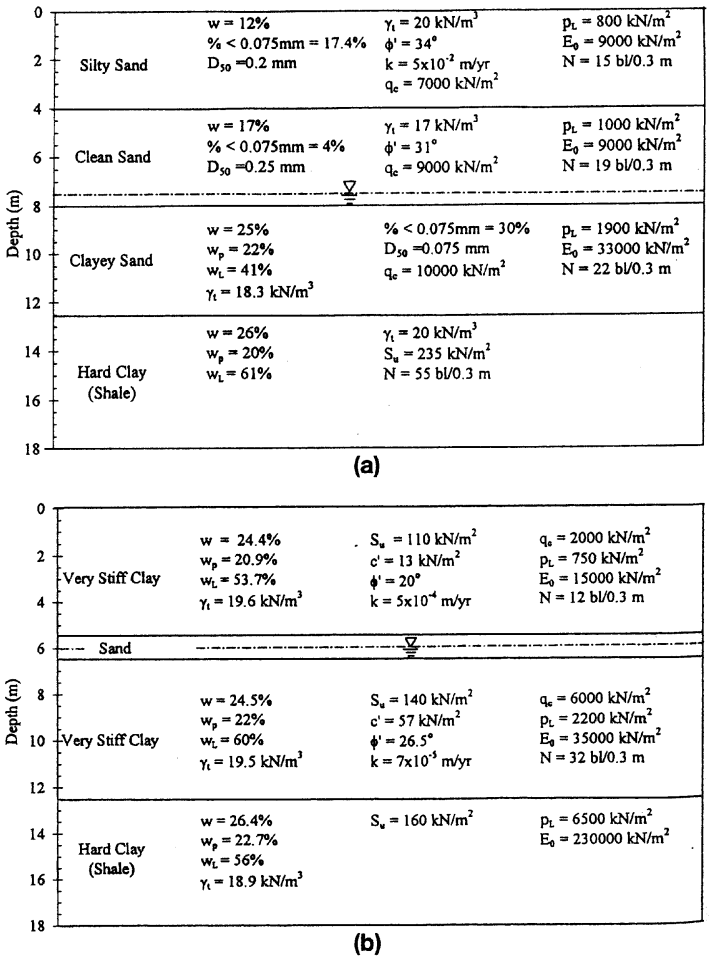

FIG. 1. Summary of Soil Properties at NGES-TAMU Sites: (a) Sand Site; (b) Clay Site

[1]Spencer J. Buchanan Prof., Dept. of Civ. Engrg., Texas A&M Univ., College Station, TX 77843-3136.

[2]Dir., Institute for Geotechnics & Materials, P.O. Box 166-864, Achrafieh, Beirut, Lebanon.

[3]Engr., 633 Bay #202, Toronto, Ontario, M5G2G4, Canada.

Note. Discussion open until December 1, 2000. To extend the closing date one month, a written request must be filed with the ASCE Manager of Journals. The manuscript for this paper was submitted for review and possible publication on January 26, 1998. This paper is part of the ***Journal of Geotechnical and Geoenvironmental Engineering***, Vol. 126, No. 7, July, 2000. ©ASCE, ISSN 1090-0241/00/0007-0640–0649/$8.00 + $.50 per page. Paper No. 17460.

TABLE 1. Construction and Testing Schedule

Pile number (1)	Site (2)	Drilling (3)	Concreting (4)	Static test 1 (5)	Statnamic test (6)	Drop weight test (7)	Static test 2 (8)
2	sand	Nov. 16, 1990	Nov. 19, 1990	Nov. 28, 1990	Dec. 4, 1990	Dec. 6, 1990	Dec. 8, 1990
4	sand	Nov. 19, 1990	Nov. 19, 1990	Nov. 30, 1990	Dec. 5, 1990	Dec. 7, 1990	—
7	clay	Nov. 15, 1990	Nov. 15, 1990	Dec. 3, 1990	Dec. 7, 1990	Dec. 8, 1990	—

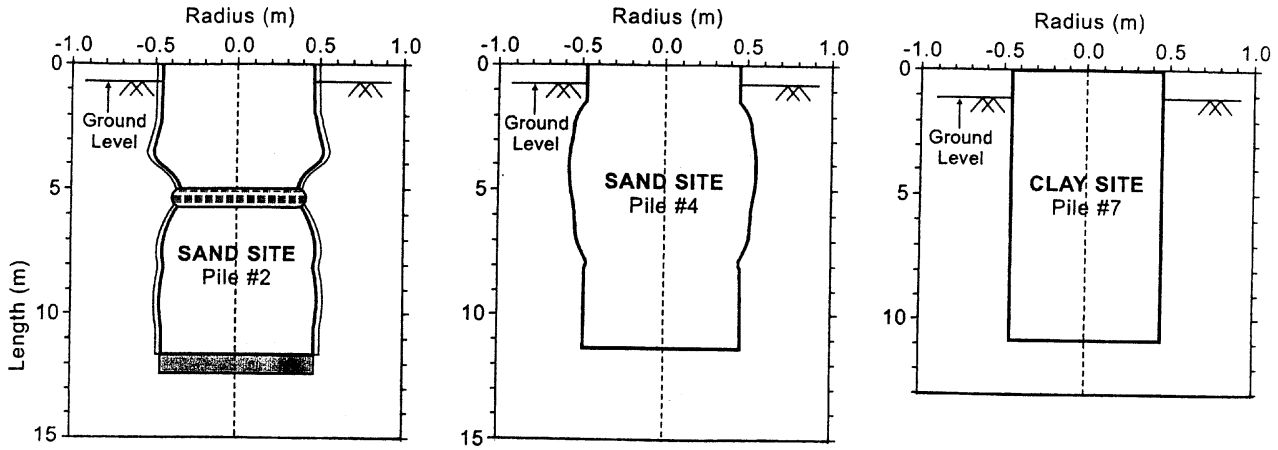

FIG. 2. Bored Piles at NGES-TAMU Sites

m-thick layer of loose clayey sand. The concrete contamination at 5.3 m occurred when the concrete tremie was purposely pulled above the concrete-mud interface during the concreting process. An unplanned defect occurred at 5.0 m below the top of the pile and resulted in a 45% necking or reduction in area.

Pile 4 (Fig. 2) at the sand site was planned as a no-defect pile with no drilling mud stagnation and proper drilling mud desanding to avoid a soft bottom; however, caving of the side walls created an unplanned bulging defect resulting in a 10% average increase in diameter between 1.2 and 7.5 m below the top of the pile.

Pile 7 (Fig. 2) at the clay site was planned and executed as a perfect pile. The shapes of piles 2, 4, and 7 as obtained from the concrete volume curves are shown in Fig. 2. Piles 2, 4, and 7 were subjected to static load testing, Statnamic testing, and drop weight testing. The testing sequence is given by the dates in Table 1.

PILE INSTRUMENTATION

In order to obtain the load distribution in the pile during the static load test, sister bars were installed. A sister bar [Fig. 3(a)] consisted of a 1.4-m-long number 4 reinforcement bar with a vibrating wire strain gauge welded to the steel in the center of the bar. The sister bars were tied to the tie bars of the reinforcement cage away from the longitudinal bars to achieve a better bonding with the concrete. In pile 2 and pile 4, the strain gauges of the sister bars were located at 3.2, 6.3, and 9.3 m below the pile top. In pile 7, they were at 4.7 and 9.2 m below the pile top. The strain gauge of each sister bar gives the strain ε in the concrete and in the steel and therefore the load P in the pile at that depth:

$$P = A_c E_c \varepsilon + A_S E_S \varepsilon \quad (1)$$

where A_c and A_S = concrete and steel cross section areas, respectively, and E_c and E_S are the concrete and steel modulus of elasticity, respectively.

Removable extensometers were also used to measure the load in the piles. Two diametrically opposed 76 mm ID PVC closed-end pipes were tied to the reinforcement cage of piles

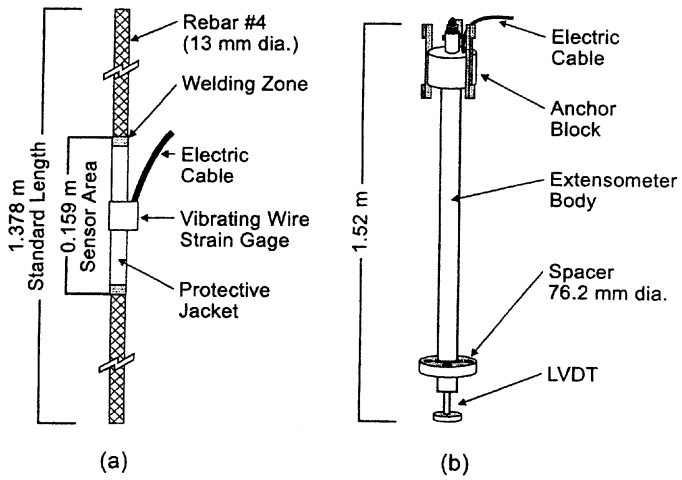

FIG. 3. Pile Instrumentation: (a) Sister Bars; (b) Removable Extensometers

2, 4, and 7. The removable extensometers [Fig. 3(b)] were 1.525 m long with an expanding anchor at one end and a displacement transducer at the other. Five extensometers were placed on top of each other in each of the two PVC pipes before the load tests. The anchors were expanded mechanically to connect the extensometers to the pile; each displacement transducer was resting on the anchor of the extensometer below it. The displacement transducer gives the change in length of the 1.525 m segment of pile and therefore the strain from which the load in the pile is calculated. The advantage of the extensometers is that they can be reused; the limitation is that the change in length of the 1.525 m segment of pile must be larger than the smallest detectable movement for the displacement transducer.

STATIC LOAD TESTS AND LOAD-SETTLEMENT CURVES

The load test setup is illustrated in Fig. 4. The load was measured by using a 10,000 kN load cell, and the displacement

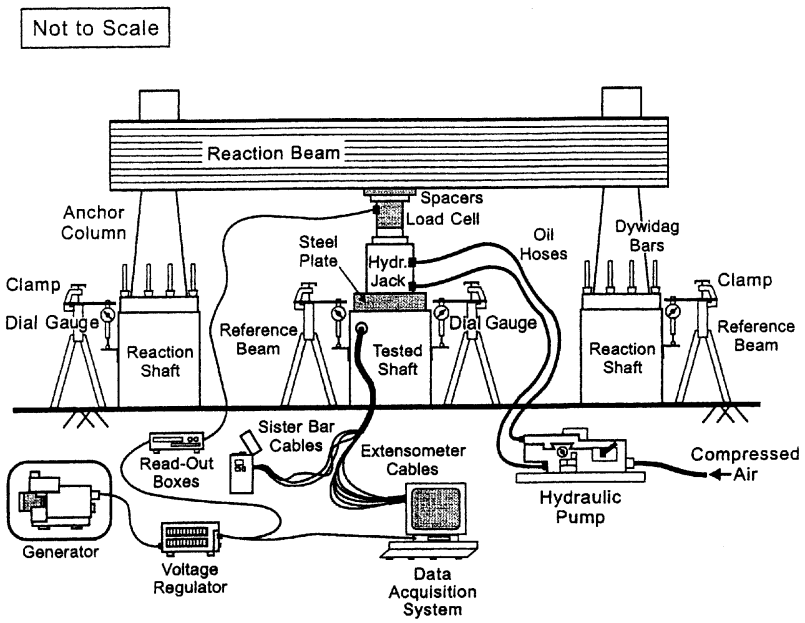

FIG. 4. Schematic View of Static Load Test

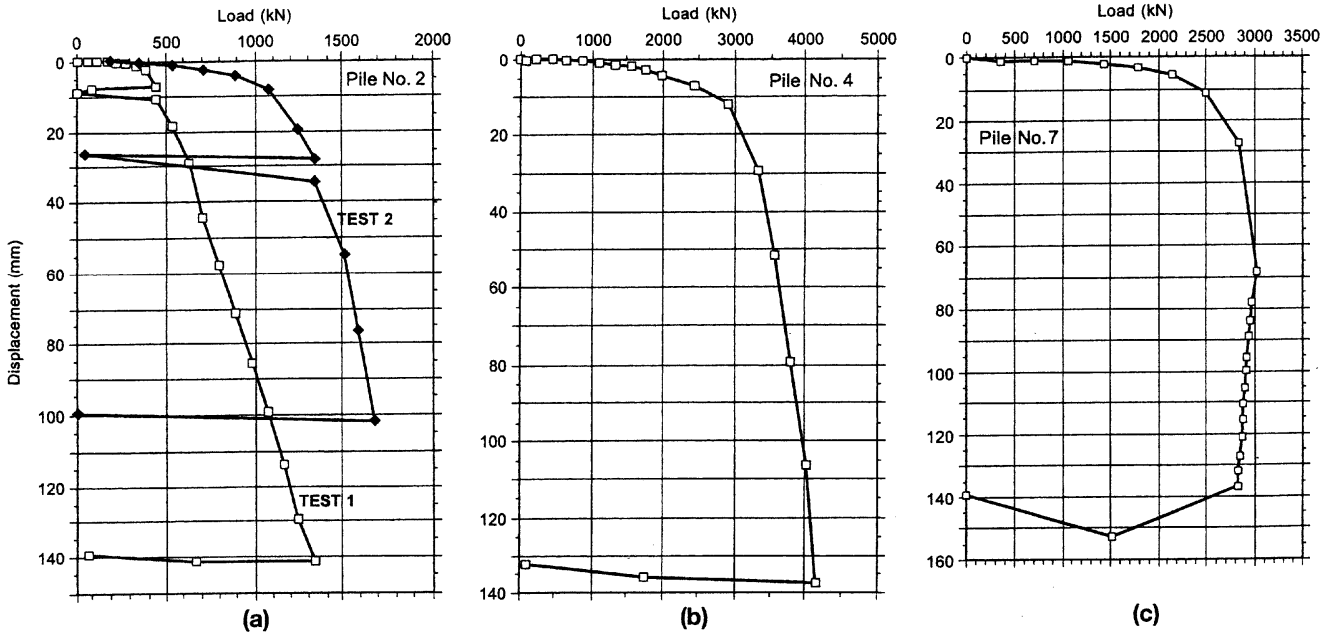

FIG. 5. Load-Settlement Curves for Static Load Tests: (a) Pile 2; (b) Pile 4; (c) Pile 7

was measured with dial gauges attached to reference beams with supports placed at least 5 pile diameters away. The strain in the sister bars and the displacement of the extensometers were also recorded during the tests.

The load was applied in a series of 15 min load steps. During each load step, the displacement and the load at the pile top, as well as the strain in the sister bars and the displacement of the extensometers, were recorded at 1, 3, 7, and 15 min. The load steps were chosen as one tenth of the estimated pile capacity and the piles were pushed to about 140 mm of penetration.

Piles 2, 4, and 7 were load tested before any dynamic tests took place. Pile 2 was subjected to a second static load test after the dynamic tests to confirm the capacity. The results of the tests are shown in Fig. 5 for the 15 min readings. There are many ways to define pile capacity from a load settlement curve (e.g., Fellenius 1975). Capacities defined according to the Davisson criterion ($D/120 + 3.8$ mm $+ PL/AE$) and the $D/10$ criterion ($D/10 + PL/AE$) are shown in Table 2. The diameter of the pile is D, the length of the pile is L, the cross section area of the pile is A, the modulus of the pile material is E, and the load applied is P. On the average, the Davisson capacity is equal to 0.72 times the $D/10$ capacity and corresponds to an average pile top penetration of 12 mm; such a small displacement is in most instances an acceptable settlement and much too small for a capacity determination. The $D/10$ criterion, on the other hand, corresponds to an average pile top penetration of 93 mm and, in the writer's opinion, should be favored for capacity determination.

LOAD DISTRIBUTION IN PILES

The load distribution in the piles was obtained separately from the sister bars and from the extensometers. The load distributions according to the sister bars for the four load tests

TABLE 2. Observations on Static Capacity of Piles

Parameters (1)	Sand Site			Clay Site
	Pile 2 (test 1) (2)	Pile 2 (test 2) (3)	Pile 4 (4)	Pile 7 (5)
Capacity ($D/10$ + PL/AE)	1,068	1,602	4,004	3,025
Capacity (Davisson)	472	1,112	2,892	2,491
Point load (kN)($D/10$ + PL/AE)	590	770	700	1,050
Friction load (kN) ($D/10$ + PL/AE)	178	832	3,304	1,975
Point pressure, q_{max} (kPa)	1,355	1,172	1,065	1,598
Friction stress, f_{max} (kPa)	5.7	26.6	108.6	71.7
q_c for point (kPa)	10,000	10,000	10,000	6,000
q_c for friction (kPa)	8,400	8,400	8,400	4,000
P_L for point (kPa)	1,900	1,900	1,900	2,200
P_L for friction (kPa)	1,100	1,100	1,100	1,475
N for point (bpf)	22	22	22	32
N for friction (bpf)	18	18	18	22
S_u for point (kPa)	—	—	—	140
S_u for friction (kPa)	—	—	—	125
σ'_{ov} for point (kPa)	159	159	156	162
σ'_{ov} for friction (kPa)	90.6	90.6	90.2	92.4
q_{max}/q_c	0.135	0.117	0.106	0.266
f_{max}/q_c	0.000679	0.00317	0.0129	0.0179
q_{max}/P_L	0.713	0.617	0.561	0.726
f_{max}/P_L	0.00518	0.0242	0.0987	0.0486
q_{max}/N	61.6	53.3	48.4	49.9
f_{max}/N	0.32	1.48	6.0	3.26
q_{max}/S_u	—	—	—	11.4
f_{max}/S_u	—	—	—	0.574
q_{max}/σ'_{ov}	8.52	7.37	6.83	9.86
f_{max}/σ'_{ov}	0.063	0.29	1.20	0.78

on the three piles are shown in Figs. 6 and 7. The distributions from the extensometers confirmed the general trend.

As can be seen from the load-settlement curves on Fig. 5, pile 2 carried much less load than pile 4 even though they have the same diameter and the same length in the same soil. The $D/10$ capacity of pile 2 is about four times smaller than the $D/10$ capacity of pile 4. The soft bottom defect on pile 2 does not seem to be a true defect, since the point loads are (Figs. 6 and 7) 880 kN for pile 2 and 700 kN for pile 4 at the $D/10$ criterion according to the sister bars. It is likely that the weight of the wet concrete recompressed the soft bottom to stiffen it back to the original condition or else the wet concrete permeated or mixed with the soft bottom and turned it into an integral part of the pile.

The friction load is much lower for pile 2 than it is for pile 4: 190 kN for pile 2 and 3,300 kN for pile 4 at the $D/10$ criterion, according to the sister bars. This very large difference is due to the mud cake and to the bulging configuration of the shaft of pile 4. The bulging of pile 4 increased the diameter from 0.915 to 1.10 m at the largest point of the bulb; this corresponds to an increase in cross-section area from 0.66 m^2 to 0.95 m^2. The increase in friction capacity due to the bulging of pile 4 can be estimated as the sum of the bearing capacity of the sand (obtained from the point measurements at the $D/10$ criterion) times the difference in area (700 kN/0.66 m^2 (0.95 − 0.66) = 307 kN) plus the increase in friction due to the increase in shaft area from a depth of 1.2 m to 7.5 m ($1.10 - 0.915/2 \times \pi(7.5 - 1.2) \times 108.6 = 199$ kN). This increase in friction (307 + 199 = 506 kN) is far from explaining much of the difference in friction between pile 2 and pile 4. Therefore, most of the loss in friction is attributed to the thick mud cake on pile 2, which decreases the friction load by a factor of about 15. This underscores the great importance of avoiding slurry stagnation.

Another observation is that the load settlement curves of the 2 bored piles in sand did not plunge while the one in clay did. Table 2 shows a number of results related to the static capacity of the piles defined at $D/10$ + PL/AE, including classical relationships to the soil parameters.

Residual stresses in bored piles after construction are usually considered to be insignificant; however, they can be induced by a load test. Residual stresses do not affect the plunging load of a pile but do affect the initial slope of the load settlement curve and the load distribution in a pile (Briaud and Tucker 1984). Static load test 2 on pile 2 started with residual stresses induced by previous testing. This is in part why the initial slope of the load settlement curve is stiffer. The load distribution shown on Fig. 6(b) does not include the residual loads; if it is assumed that the point and friction loads for test 2 are the same as for test 1, the residual point load in test 2 is 180 kN [1,000 kN (820 kN on Fig. 6)] or about 18% of the

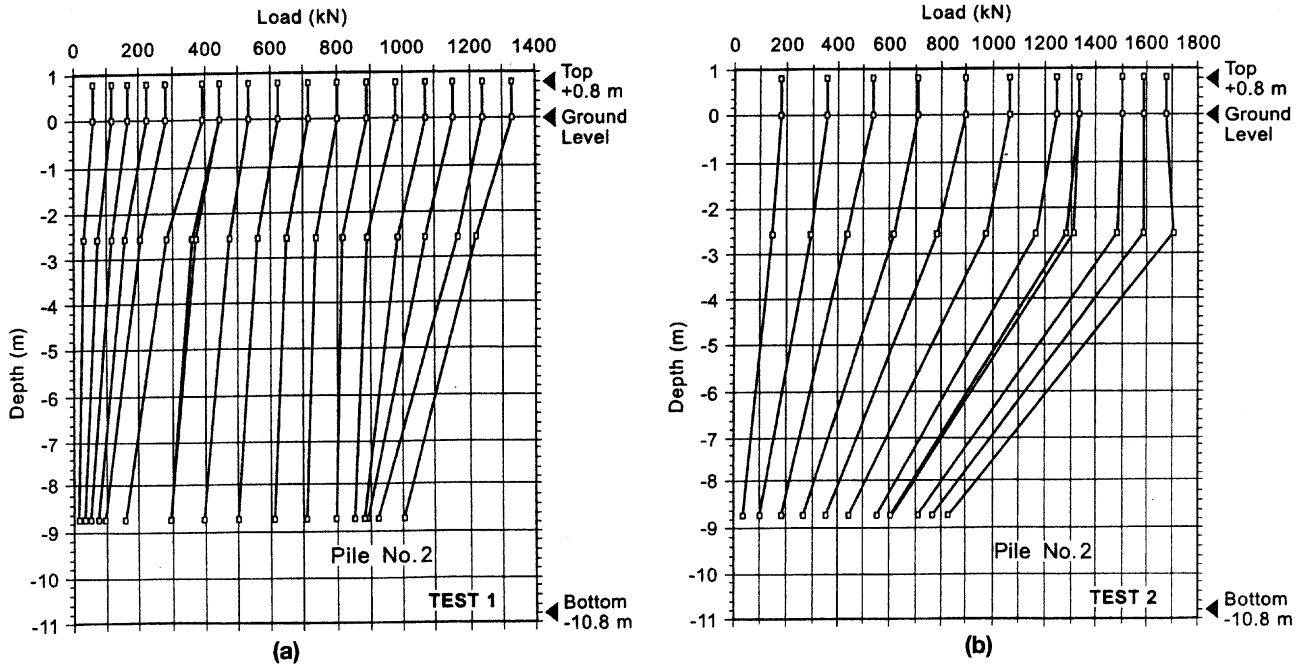

FIG. 6. Load versus Depth Profiles for Pile 2: (a) Test 1; (b) Test 2

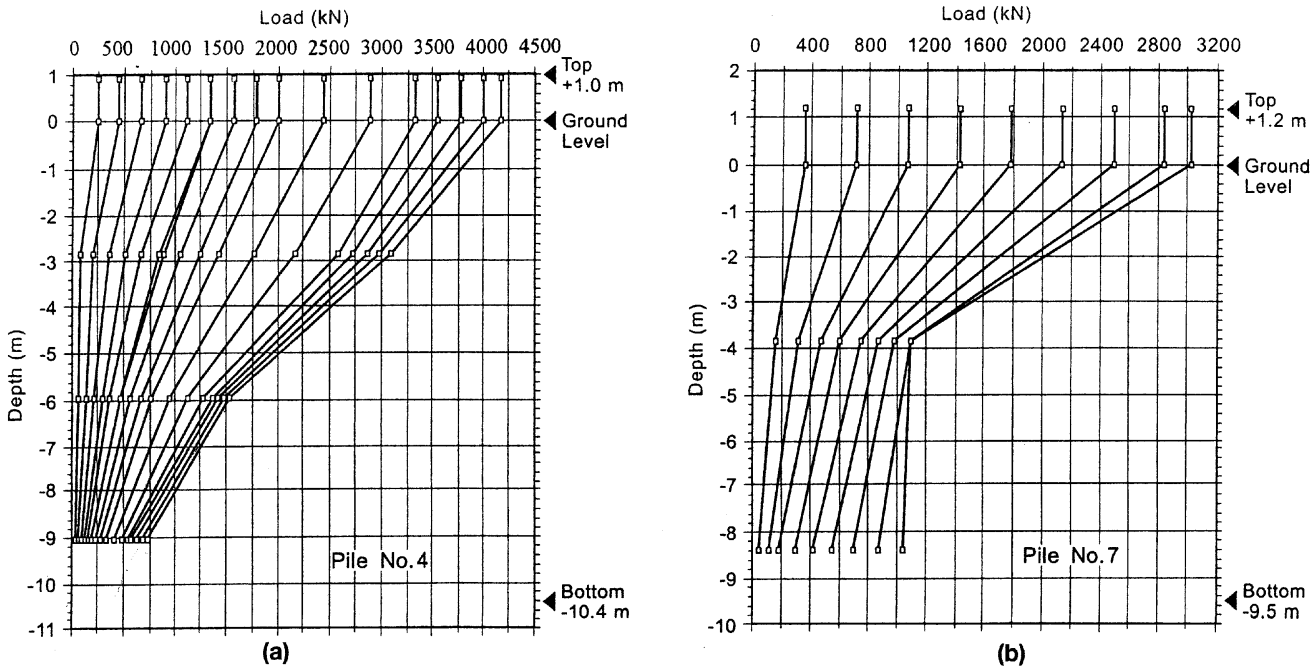

FIG. 7. Load versus Depth Profiles for (a) Pile 4; (b) Pile 7

point load. This is consistent with previous findings (Briaud and Tucker 1984a).

STATNAMIC TESTING

The Statnamic test [Bermingham and Janes 1989; Horvath et al. 1990; El Naggar and Novak (1991 (Fig. 8)] was performed by the Berminghammer Corporation (Berninghammer 1991). The test consists of placing a reaction mass on top of the bored pile to be tested. Between the pile and the reaction mass are a load cell and a fuel chamber. The solid fuel propellant is ignited and propels the reaction mass upward (from

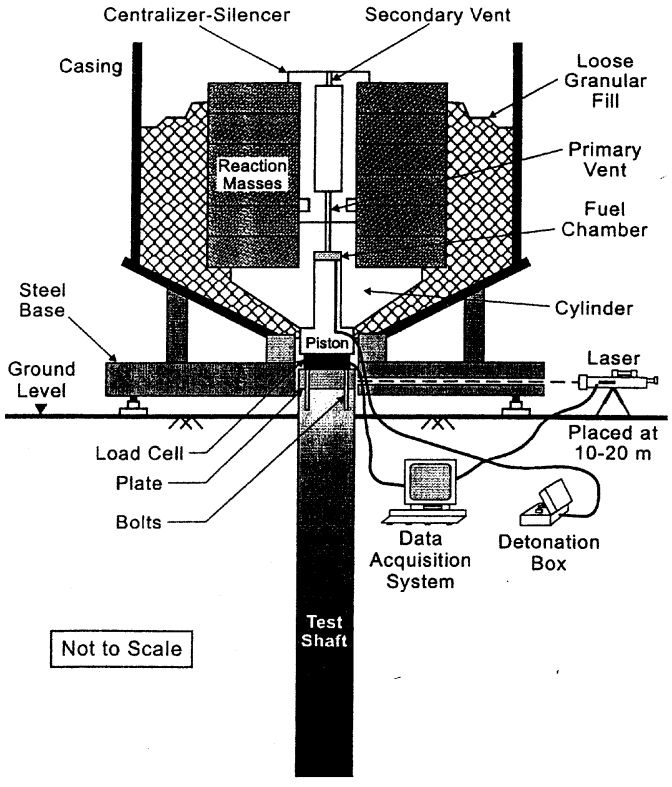

FIG. 8. Schematic View of Statnamic Test

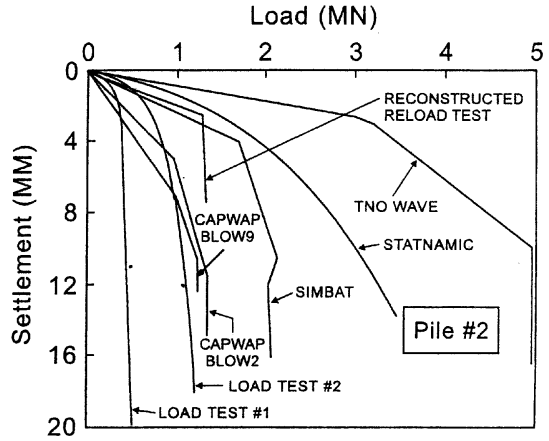

FIG. 9. Comparison between Measured and Predicted Static Load-Settlement Curves for Pile 2

1 to 3 m) while pushing the bored pile downward (from 10 to 100 mm). The loading part of the event lasts about 50 milliseconds, during which both load and displacement are recorded. The load is obtained from the load cell and the displacement is measured with a remote laser light source stationed 10 to 20 m away to minimize ground vibration; the laser beam hits a light-sensitive cell placed on the pile. The result of the test in the field is a dynamic load-settlement curve. A static load-settlement curve is then generated from the dynamic curve (Berminghammer 1991).

The Statnamic tests were performed from four to seven days after the static load tests (Table 1). The static load-settlement curves are shown in Figs. 9–11. The total penetrations varied from 13 mm for pile 7 to over 70 mm for pile 2. The maximum velocities varied from 0.32 m/s for pile 7 to 2.37 m/s for pile 2. The predictor was asked to give his best estimate of the static capacity for the piles based on his own data; these values are listed in Table 3 together with the measured static capacities according to the $D/10 + PL/AE$ criterion. The predictions for pile 4 and pile 7 are relatively close, while the predicted static capacity for the unusual pile 2 is very large. Note that a proper comparison should compare the last load applied during the preceding static test rather than the $D/10$

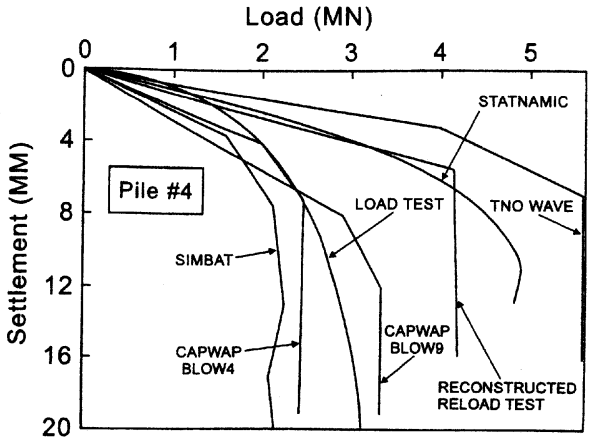

FIG. 10. Comparison between Measured and Predicted Static Load-Settlement Curves for Pile 4

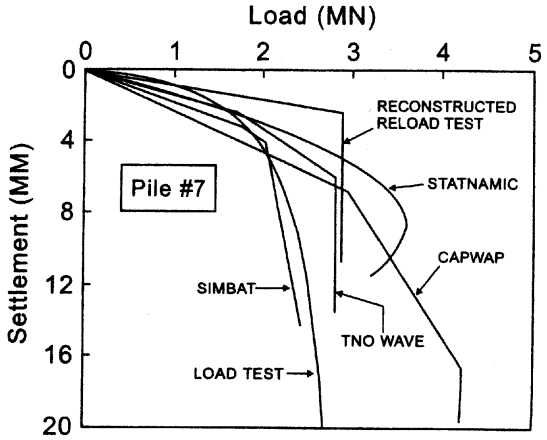

FIG. 11. Comparison between Measured and Predicted Static Load-Settlement Curves for Pile 7

TABLE 3. Comparison of Static Capacity Predictions

Parameters (1)	Sand Site		Clay Site
	Pile 2 (2)	Pile 4 (3)	Pile 7 (4)
Load at $D/10$ + PL/AE in static load test (kN)	1,068	4,004	3,025
Load at end of static load test before unloading (kN)	1,320	4,200	2,650
Load at $D/10$ + PL/AE in static load test 2 (kN)	1,602	—	—
Load at end of static load test 2 before unloading (kN)	1,680	—	—
Static capacity according to Statnamic predictor (kN)	2,460	4,490	3,150
Maximum load on static curve predicted by Statnamic test (kN)	3,600	4,900	3,600
Maximum load applied during Statnamic test (kN)	4,100	5,600	4,600
Viscous exponent, n	0.089	0.022	0.046
CASE method prediction: average of all blows (kN)	1,550	2,850	2,830
CASE method prediction for highest energy blows (kN)	1,905	3,570	3,990
CAPWAP prediction: average of two runs (kN)	1,300	2,900	4,250
TNOWAVE prediction (kN)	4,900	5,800	2,850
SIMBAT prediction (kN)	2,100	2,300	2,500

load. Indeed, the Statnamic test was performed after the load test and therefore represents a reload cycle and not an initial loading (Table 3).

RATE EFFECT AND INERTIA EFFECT IN STATNAMIC TESTS

The load-settlement curve measured during a Statnamic test represents one cycle of quick loading; the maximum load in that cycle is called Q_{DP}, where D stands for dynamic and P for peak. The time t_D to reach Q_{DP} is relatively short; in these tests t_D was approximately 50 ms. The static capacity in the static load test is called Q_{SP}, where S stands for static. The time t_S to reach Q_{SP} is much longer; in these tests, t_S was approximately 17,000 s at the sand site and 9,000 s at the clay site. Briaud and Garland (1985) have proposed a model for rate effect:

$$\frac{Q_{DP}}{Q_{SP}} = \left(\frac{t_D}{t_S}\right)^n \tag{2}$$

where n = viscous exponent, and n varies from 0.01 for clean silica sands to 0.1 for very soft high plasticity clays. Site-specific values of n can be obtained by performing creep pressuremeter tests or cone penetrometer tests at significantly different rates of penetration. The values of n [back-calculated by using the maximum load applied during Statnamic (Q_{DP})], the maximum load applied during the first static test (Q_{SP}), and the times t_D and t_S previously mentioned are shown in Table 3. The value of 0.089 for test 2 is very high but not surprising, because the bentonite cake is equivalent to having a very soft high plasticity clay. The values of 0.022 in the silty sand and 0.046 at the clay site are very reasonable and close to measured values in other projects at the sites (Briaud 1997).

The inertia effects in a Statnamic test are usually small when the pile is close to the peak load. Indeed the average acceleration of the top of the bored piles close to the peak load varied between 0 and 1 g. In other words, the load correction on the peak load due to inertia effects is at most equal to the weight of the pile. At the beginning of the test, however, the acceleration can reach 10 g.

DROP WEIGHT TESTS

After the Statnamic tests, three companies from France/U.K., the Netherlands, and the United States were invited to come, place their instruments on the three bored piles, and give their predictions of the pile static capacity on the basis of the data collected during a drop weight program. The companies were ESSI-Testconsult (1991), GRL and Associates, Inc. (1991), and TNO Building and Construction Research (1991).

The arrangement for the drop weight tests is illustrated in Fig. 12. The ground around the shaft was excavated down to 1.6 m below the ground surface, thus allowing each company to place their own combination of accelerometers and strain gauges at about 1.5 m below the pile top. An electronic theodolite was also placed by ESSI-Testconsult about 15 m away from the pile together with a target on the pile to continuously record the dynamic displacement of the pile associated with each blow.

The hammer had a ram weighing about 90 kN and the falling height was varied from 0.3 to 5 m. Because of the friction in the leads, the energy required to accelerate the cable hoist, and the cushion placed between the ram and the pile top, the actual energy delivered to the pile head was about 20% of the free fall energy of the ram. The delivered energy during the series of blows with varying drop height ranged from 7 to 90 kJ and caused the permanent displacement per blow of the piles to vary from a fraction of 1 mm to 13 mm per blow.

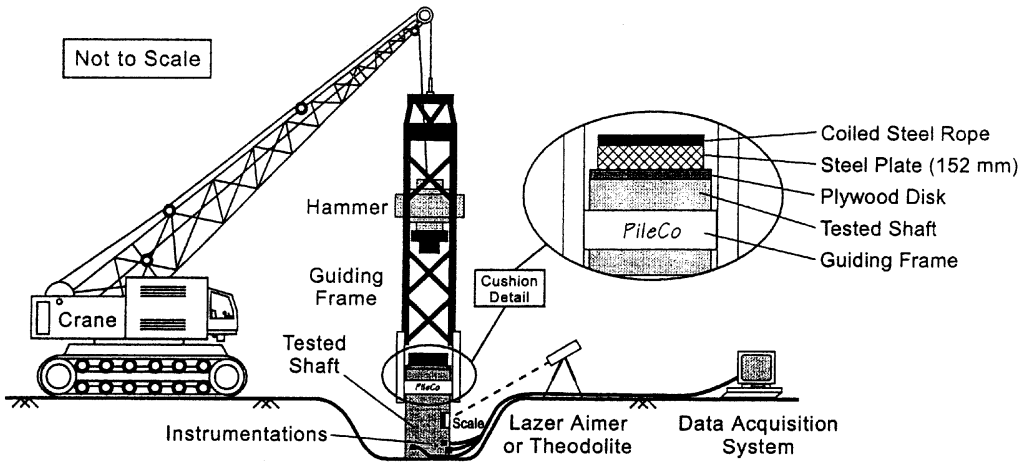

FIG. 12. Schematic View of Drop Weight Test

PREDICTIONS OF STATIC CAPACITY FROM DROP WEIGHT TESTS

The data obtained by each company for each blow was similar. It consisted of the force-time signal from the strain gauges, the acceleration-time signal from the accelerometers, and the permanent displacement of the pile top. A series of blows was applied to the pile top by varying the height of drop.

The methods used to predict the static capacity and the load-settlement curve are significantly different from one company to another. GRL uses the case method (Goble et al. 1970) and the CAPWAP method (Rausche et al. 1972; CAPWAP 1997); ESSI-Testconsult uses the SIMBAT method (Paquet 1988; Stain and Davis 1989); and TNO uses the TNOWAVE method (Middendorp and VanWeele 1986; TNOWAVE 1997).

The results of the predictions for static capacity are presented in Table 3. For the CASE method a static capacity is predicted for each blow. Since several blows with different drop heights were applied to the piles, several CASE method predictions were made. Table 3 shows the average of those predictions. Fig. 13(a) shows the CASE method predictions as a function of the permanent set; the permanent set is defined as the difference in elevation of the pile top before and after the blow.

It is clear from Fig. 13(a) that the static capacity predicted by the CASE method increases with the permanent set. Indeed the CASE method will predict a load associated with the amount of movement generated during the blow. The SIMBAT method does acknowledge the fact that different impact energies will lead to different points on the curve; in fact it takes advantage of that by using a series of blows with varying energy to describe the complete curve. The blow count is equal to 300 mm divided by the permanent set and is shown on Fig. 13(a). Hammer size is relative to pile size and resistance. Hammers that are larger than required will generate large permanent sets and low blow counts, while hammers that are smaller than required will lead to small permanent sets and high blow counts. Fig. 13 shows, therefore, that large hammers will lead to large predicted pile capacities and small hammers will lead to small predicted pile capacities. More accurately, large hammers are likely to lead to loads corresponding to large pile displacements, while small hammers are likely to lead to loads corresponding to small pile displacements [Fig. 13(b)].

In order to evaluate the predicted static capacities, one must determine which measured load to compare them to. The static capacity according to Davisson's criterion is not selected, because it corresponds to too small a settlement. The load according to the $D/10$ criterion could be selected, but the last load applied to the pile during the static load test is preferred

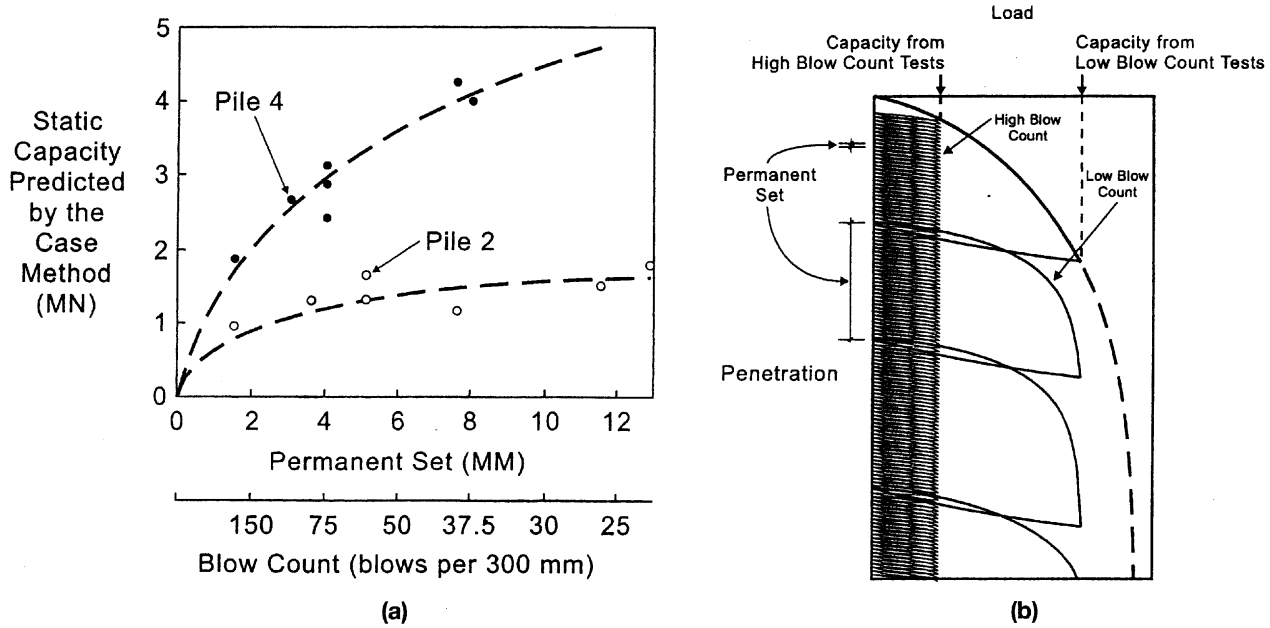

FIG. 13. Influence of Blow Count on Capacity: (a) Case Method; (b) Illustration

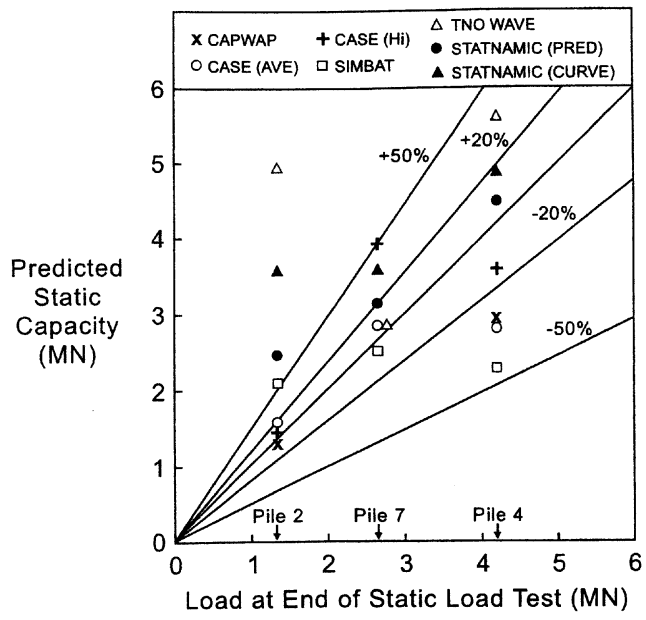

FIG. 14. Comparison between Predicted and Measured Static Capacities

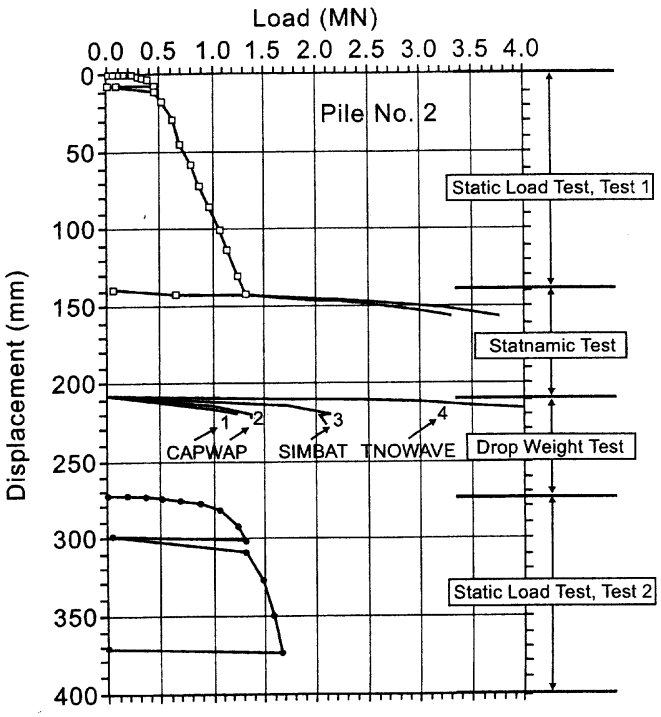

FIG. 15. Complete Load-Settlement History for All Tests on Pile 2

because in this research project the dynamic tests were in fact reload tests that occurred after the end of the static test. The comparison is shown in Fig. 14. The scatter is narrower for the piles in clay than for the two piles in sand. Also, some methods show less scatter than others.

LOAD-SETTLEMENT CURVES

One way to avoid having to choose which static capacity should be used to compare with the predicted static capacities is to compare the complete load-settlement curves. The CAPWAP, SIMBAT, and TNOWAVE methods do predict the complete static load-settlement curve. CAPWAP and TNOWAVE base their predictions on a signal matching process and therefore make one complete load-settlement curve prediction for each blow. SIMBAT, on the other hand, bases its prediction on a series of blows of varying drop height and makes one prediction for a series of blows.

Again the problem arises of knowing which measured load-settlement curve should be used for comparison purposes. The initial loading curve of the load test can be used but it is not the one that corresponds to the drop weight test, since the pile is actually being reloaded by the drop weight test. A more appropriate load-settlement curve would be one that would correspond to a reload cycle performed at the end of the static load test; unfortunately, such an unload-reload cycle was not performed during the load tests on piles 4 and 7. The curves identified as reconstructed reload test on Figs. 9–11 were obtained by using an initial slope equal to the slope of the unload curve at the end of the load test and switching at the last load applied in the load test to a slope equal to the slope of the load-settlement curve at the end of the test. For pile 2 a second load test was performed after the drop weight tests. Figs. 9–11 show the comparison between the load-settlement curves. Fig. 15 shows the complete sequence of tests of pile 2.

Another issue is the setup factor, since the static and dynamic load tests were performed at different times after the construction of the bored piles. This is not thought to be a major issue because these piles are bored piles, not driven piles, and because two of them are in sand. Furthermore, static test 2 on pile 2 was performed 10 days after the static test 1 and after the Statnamic test and the drop weight test; yet inspection of Fig. 5(a) shows that the load-settlement curve of static test 2 fits very well as a continuation of the load-settlement curve of static load test 1. No data exists to evaluate the setup on pile 7 at the clay site.

Figs. 9–11 lead to the following observations. First, the scatter in the predictions decreases from pile 2 to pile 4 and then to pile 7, which shows relatively good agreement between all predictions. Second, the working load to be applied to the pile can be chosen as one-half the static capacity obtained on the static load-settlement curve predicted from a dynamic load test; the values obtained with such a definition are shown in Table 4. These values are equal to one half of the values shown in Table 3. The actual settlement, s, which would take place under these working loads, and the actual factor of safety F for each one of these working loads are also shown in Table 3. Note that s can be read on the original load test curve or on the reconstructed load curve. Furthermore, F can be taken as the ratio of the working load over the $D/10$ static capacity from the static load test or over the load applied at the end of the static load test. The average settlements and factors of safety shown in Table 4 indicate that the dynamic tests lead to satisfactory recommendations for piles 4 and 7 for all methods, to satisfactory recommendations for pile 2 for some methods, and to unsatisfactory recommendations for pile 2 for other methods. These tests represent one indication that these dynamic methods are satisfactory for routine conditions but that some dynamic methods need refinement for unusual conditions.

CONCLUSIONS

The following conclusions are based on static load tests, Statnamic tests, and drop weight tests on two bored piles in sand and one bored pile in clay. While it is not possible to make general conclusions with experiments on only three bored piles, it is also impossible to ignore these results.

1. In the static load tests, the static capacity is defined as the load corresponding to a settlement equal to $D/10 + PL/AE$. For this load a series of useful ratios between, on one hand, the shear stress at the soil-pile interface and the pressure under the pile point, and on the other hand, various soil properties are presented in Table 2.

TABLE 4. Observations at Working Loads

Parameters (1)	Sand Site		Clay Site
	Pile 2 (2)	Pile 4 (3)	Pile 7 (4)
Q_1 = 1/2 the $D/10$ load from static test (kN)	534	2,002	1,512
Q_2 = 1/2 the load at the end of static test (kN)	660	2,100	1,325
Q_3 = 1/2 the static capacity according to STATNAMIC predictor (kN)	1,230	2,245	1,575
Q_4 = 1/2 the maximum load reached on the predicted static curve from STATNAMIC (kN)	1,800	2,450	1,800
Q_5 = 1/2 the CASE static capacity (average of all blows) (kN)	775	1,425	1,415
Q_6 = 1/2 the CASE static capacity for highest blows (kN)	952	1,785	1,995
Q_7 = 1/2 the CAPWAP static capacity (kN)	650	1,450	2,125
Q_8 = 1/2 the TNOWAVE static capacity (kN)	2,450	2,900	1,425
Q_9 = 1/2 the SIMBAT static capacity (kN)	1,050	1,150	1,250
S_{31} = settlement for Q_3 on static test curve (mm)	130	5.5	2
S_{41} = settlement for Q_4 on static test curve (mm)	>140	7	3.5
S_{51} = settlement for Q_5 on static test curve (mm)	67	1.6	1.8
S_{61} = settlement for Q_6 on static test curve (mm)	80	3	4.6
S_{71} = settlement for Q_7 on static test curve (mm)	35	2	5.6
S_{81} = settlement for Q_8 on static test curve (mm)	>140	13.5	2
S_{91} = settlement for Q_9 on static test curve (mm)	90	1	1.3
S_{32} = settlement for Q_3 on static reload curve (mm)	2.3	5.5	2.2
S_{42} = settlement for Q_4 on static reload curve (mm)	>140	3.3	1.4
S_{52} = settlement for Q_5 on static reload curve (mm)	1.5	2	1
S_{62} = settlement for Q_6 on static reload curve (mm)	1.9	24	1.6
S_{72} = settlement for Q_7 on static reload curve (mm)	1.3	2	1.7
S_{82} = settlement for Q_8 on static reload curve (mm)	>140	3.8	1.1
S_{92} = settlement for Q_9 on static reload curve (mm)	2	1.5	1
F_{31} = factor of safety $2Q_1/Q_3$	0.87	1.78	1.92
F_{41} = factor of safety $2Q_1/Q_4$	0.59	1.63	1.68
F_{51} = factor of safety $2Q_1/Q_5$	1.38	2.81	2.14
F_{61} = factor of safety $2Q_1/Q_6$	1.12	2.24	1.52
F_{71} = factor of safety $2Q_1/Q_7$	1.64	2.76	1.42
F_{81} = factor of safety $2Q_1/Q_8$	0.44	1.38	2.12
F_{91} = factor of safety $2Q_1/Q_9$	1.02	3.48	2.42
F_{32} = factor of safety $2Q_2/Q_3$	1.07	1.87	1.68
F_{42} = factor of safety $2Q_2/Q_4$	0.73	1.71	1.47
F_{52} = factor of safety $2Q_2/Q_5$	1.70	2.95	1.87
F_{62} = factor of safety $2Q_2/Q_6$	1.39	2.35	1.33
F_{72} = factor of safety $2Q_2/Q_7$	2.03	2.90	1.25
F_{82} = factor of safety $2Q_2/Q_8$	0.54	1.45	1.86
F_{92} = factor of safety $2Q_2/Q_9$	1.26	3.65	2.12
Average settlement on static test curve (mm)	>97.4	4.80	3.0
Average settlement on reload test curve (mm)	>41.3	2.90	1.40
Average factor of safety against $2Q_1$	1.01	2.30	1.89
Average factor of safety against $2Q_2$	1.25	2.41	1.65

2. The comparison between the last load applied in the static load test (settlement ~140 mm) and the static capacity predicted from the dynamic load tests shows narrower scatter for the pile in clay than for the piles in sand. Also, some methods show less scatter than others (Fig. 14).
3. If the dynamic methods had been used to determine the static capacity and if a load equal to one half of that static capacity (factor of safety of 2) had been chosen as a working load, piles 4 and 7 would have performed satisfactorily (average settlement <5mm, average factor of safety >1.65) while pile 2 would have performed satisfactorily for some methods but not for others.
4. The tests on these three bored piles are an indication that while dynamic methods do not give a consistently accurate prediction of static capacities they do lead to generally acceptable working loads for piles without unusual conditions (piles 4 and 7). Some dynamic methods need to be improved to predict the behavior of unusual piles like pile 2.

ACKNOWLEDGMENTS

Many individuals and organizations have contributed to this project. They are all thanked very sincerely. The major sponsors of the study are the Federal Highway Administration with Carl Ealy and Al Dimillio, and the ADSC with Scott Litke, Gus Beck, Keith Anderson, and J. Clayton Stevens. The project was administered by PSC with Gary Parikh and Francis Mensah. Many other organizations have contributed financially to this project, including Drillers Inc./Farmer, PileCo, Lewis Inc., A. H. Beck Foundation Co., Polymer Drilling Services, Goble Rausche Likins, ESSI-Testconsult, STS Consultants, TNO, Olson Engineering, Berminghammer, the University of Houston, Texas A&M University, and Briaud Engineers.

APPENDIX. REFERENCES

Baker, C. N., Parikh, G., Briaud, J.-L., Drumright, E. E., and Mensah-Dwumah, F. (1993). "Drilled shafts for bridge foundations." *Rep. No. FHWA-RD-92-004*, Federal Highway Administration, Washington, D.C., 335.

Ballouz, M., Nasr, G., and Briaud, J.-L. (1991). "Dynamic and static testing of nine drilled shafts at Texas A&M University geotechnical sites." *Res. Rep.*, Civil Engineering, Texas A&M University, College Station, Tex., 127.

Bermingham, P., and Janes, M. (1989). "An innovative approach to load testing of high capacity piles." *Proc., Int. Conf. on Piling and Deep Found.* J. B. Burland and J. M. Mitchell, eds., Balkema, Rotterdam, The Netherlands, 409–413.

Berminghammer Corporation Ltd. (1991). "Statnainic load test results—Texas A&M University—comparative pile foundation load test program, Berminghammer Corp. Ltd." *Rep. dated January 14, 1991*, Berminghammer Corporation Ltd., Hamilton, Ont.

Briaud, J.-L. (1997). "The national geotechnical experimentation sites at Texas A&M University: Clay and sand—a summary." *Rep. NGES-TAMU-007*, Civil Engineering, Texas A&M University, College Station, Tex., 34.

Briaud, J.-L., and Garland, E. (1985). "Loading rate method for pile response in clay." *J. Geotech. Engrg.*, ASCE, 111(3), Reston, Va., 319–335.

Briaud, J.-L., and Tucker, L. M. (1984). "Piles in sand: A method including residual stresses." *J. Geotech. Engrg.*, ASCE, 110(11), 1666–1680.

Briaud, J.-L., and Tucker, L. M. (1984a). "Residual stresses in piles and the wave equation." *Proc., Symp. on Deep Found.*, ASCE, New York.

El Naggar, M. H., and Novak, M. (1991). "Analytical model for an innovative pile test." *Geotech. Res. Ctr. Rep. GEOT-7-91*, Faculty of Engineering Science, University of Western Ontario, London, Canada, 35.

ESSI-Testconsult. (1991). "Dynamic testing of drilled shafts by the SIMBAT method." *Report no. 58/91*, Skokie, Ill., p. 8.

Fellenius, B. H. (1975). "Test loading of piles and new proof testing procedure." *J. Geotech. Engrg. Div.*, ASCE, 101(9), 855–869.

Goble, G. G., Rausche, F., and Moses, F. (1970). "Dynamic studies on the bearing capacity of piles—phase III." *Final Rep. to the Ohio Department of Highways*, Case Western Reserve University, Cleveland, Ohio.

GRL and Associates, Inc. (1991). Drilled shaft test program—Texas A&M University, *GRL Job No. 916008*, Cleveland, Ohio, p. 9.

GRL & Associates. (1997). *GRL software: Case pile wave analysis program (CAPWAP)*. Cleveland, Ohio.

Horvarth, R. C., Bermingham, P., and Janes, M. (1990). "The Statnamic loading test, an innovative method for predicting capacity of deep foundations." *Proc., 43rd Can. Geotech. Conf.*, Laval University, Quebec, Canada, 143–150.

Middendorp, P., and Van Weele, A. F. (1986). "Application of characteristic stress wave method in offshore practice." *Proc. 3rd Int. Conf. on Numer. Methods in Offshore Piling*, Editions Technip, Paris.

Paquet, J. (1988). "Checking bearing capacity by dynamic loading—choice of a method." *Proc., 3rd Int. Conf. on the Appl. of Stress Wave Theory to Piles*, B. H. Fellenius, ed., Bitech Publishers, Vancouver, Canada.

Rausche, F., Moses, F., and Goble, G. (1972). "Soil resistance predictions from pile dynamics." *J. Soil Mech. and Found. Div.*, ASCE, 98(9), 917–938.

Simon, P., and Briaud, J.-L. (1996). "The national geotechnical experimentation sites at Texas A&M University: Clay and sand-soil data in electronic form 1995–1996." *Rep. NGES-TAMU-006*, Civil Engineering, Texas A&M University, College Station, Tex., p. 43.

Stain, R. T., and Davis, A. G. (1989). "An improved method for the prediction of pile bearing capacity from dynamic testing." *Proc., Int. Conf. on Piling and Deep Found.*, J. B. Burland and J. M. Mitchell, eds., Balkema, Rotterdam, The Netherlands, 429–433.

TNO Building and Construction Research. (1991). "Dynamic load testing, FHWA test program." *TNO Rep. Memo CONSTR-91-652/MPP/MNL for Proj. No. 64.6.8000*, Delft, The Netherlands, p. 67.

TNO Building and Construction Research. (1997). *TNO software for pile driving analysis (TNOWAVE)*, Delft, The Netherlands.